Accepted Manuscript

Divergent evolution of medusozoan symmetric patterns: Evidence from the microanatomy of Cambrian tetramerous cubozoans from South China

Jian Han, Shin Kubota, Guoxiang Li, Qiang Ou, Xing Wang, Xiaoyong Yao, Degan Shu, Yong Li, Kentaro Uesugi, Masato Hoshino, Osamu Sasaki, Harumasa Kano, Tomohiko Sato, Tsuyoshi Komiya

Please cite this article as: Han, Jian, Kubota, Shin, Li, Guoxiang, Ou, Qiang, Wang, Xing, Yao, Xiaoyong, Shu, Degan, Li, Yong, Uesugi, Kentaro, Hoshino, Masato, Sasaki, Osamu, Kano, Harumasa, Sato, Tomohiko, Komiya, Tsuyoshi, Divergent evolution of medusozoan symmetric patterns: Evidence from the microanatomy of Cambrian tetramerous cubozoans from South China, *Gondwana Research* (2015), doi: 10.1016/j.gr.2015.01.003

Divergent evolution of medusozoan symmetric patterns: Evidence from the microanatomy of Cambrian tetramerous cubozoans from South China

Jian Han[a*], Shin Kubota[b], Guoxiang Li[c], Qiang Ou[d], Xing Wang[a], Xiaoyong Yao[e], Degan Shu[a], Yong Li[e], Kentaro Uesugi[f], Masato Hoshino[f], Osamu Sasaki[g], Harumasa Kano[g], Tomohiko Sato[h], Tsuyoshi Komiya[h]

[a]Early Life Institute, Department of Geology, and State Key Laboratory of Continental Dynamics, Northwest University, Xi'an 710069, China

[b]Seto Marine Biological Laboratory, Field Science Education and Research Center, Kyoto University, Shirahama, Wakayama 649-2211, Japan

[c]State Key Laboratory of Palaeobiology and Stratigraphy, Nanjing Institute of Geology and Palaeontology, Chinese Academy of Sciences, Nanjing 210008, China

[d]Early Life Evolution Laboratory, School of Earth Sciences and Resources, China University of Geosciences, Beijing 100083, China

[e]School of Earth Science and Land Resources, Key Laboratory of Western China's Mineral Resources and Geological Engineering, Ministry of Education, Chang'an University, Xi'an 710054, China

1

[f]Japan Synchrotron Radiation Research Institute (JASRI) 1-1-1 Kouto, Sayo-cho,

Sayo-gun, Hyogo, Japan

[g]Tohoku University Museum, Tohoku University, 6-3 Aoba, Aramaki, Aoba-ku,

Sendai, Japan

[h] Department of Earth Science and Astronomy, Graduate School of Arts and Sciences,

The University of Tokyo, Tokyo 153-8902, Japan

* To whom correspondence should be addressed. E-mail: elihanj@nwu.edu.cn (J.

Han)

1. Abstract

Living medusozoans and their Middle Cambrian ancestors are characterized

fundamentally by four-fold symmetry. The symmetric pattern of their earlier

antecedents during the Ediacaran-Cambrian transition, traditionally expected to be

tetramerous, need to be reconsidered in the light of Cambrian pentamerous fossil

medusozoans. Here we present a microanatomic analysis of three tiny tetramerous

specimens from the Lower Cambrian Kuanchuanpu Formation in southern China;

they display diagnostic characteristics of Cubomedusae, including paired but

well-separated interradial tentacles deep in the subumbrellar cavity, interradial septa

connected by claustra, coronal muscles at the subumbrella, and an annular velarium

suspended by twelve frenula. These fossils likely represent three new taxa of a

monophyletic stem group of cubomedusans, which is further confirmed by our phylogenetic analysis based on the data matrix with 25 taxa and 107 characteristics. Among these fossil cubozoans and co-occurring pentamerous forms, the specimen ELISN31-31 is mostly close to the crown-group Cubomedusae with regard to its narrow vascular cavity and the endodermic perradial fusion. Diverse symmetrical patterns among different lineages of Cambrian medusozoan candidates might have been independently evolved in different classes of medusozoans.

Keywords: Early Cambrian; Kuanchuanpu Formation; tetra-radial symmetry; cubozoan; embryos

2. Introduction

The Cambrian explosion is one of the most significant changes determining the entire course of animal evolution in the Phanerozoic. In the fossil records, the appearance of metazoan phyla macroevolutionary event was obviously diachronous, with three major phases (Shu et al., 2014). The third, also the largest phase occurred in the Cambrian Stage 3, which is represented by the ecological dominance of triploblastic bilaterians and minor cnidarians (Shu et al., 2014; Zhang et al., 2014). In the sights of paleontologists, the first stage (Fortunian) of Cambrian is the most crucial episode to trace the sporadic sparks of bilaterians, especially ecdysozoans and deuterostomians. However, the biological world in the Fortunian Stage, generally known as low diversity of small shelly fossils (SSFs)(Li et al., 2007a; Maloof et al.,

3

2010), is poorly understood by usually teemed with skeletonized cnidarian candidates and lophotrochozoans (Kouchinsky et al., 1999; Li et al., 2007a). The exceptionally well-preserved lagerstätte, the Kuanchuanpu Formation in Ningqiang (Fortunian Stage, *ca.* 535Ma), South China, additionally reveals a much-higher disparity of soft-bodied cnidarians (Han et al., 2013; Han et al., 2010; Steiner et al., 2014), cycloneurians, and problematic arthropods (Steiner et al., 2014), thus it provides an opportunity to unravel the co-evolution of cnidarians and bilaterians, and also insights to seek the origin and early evolution of major lineages of cnidarians (anthozoans and medusozoans).

The morphological and molecular phylogenetic relationships among their four major groups of living medusozoans (i.e. hydrozoans, staurozoans, scyphozoans, and cubozoans) are still contentious (Collins, 2002; Collins, 2009; Collins et al., 2006; Kayal et al., 2013; Marques and Collins, 2004; Thiel, 1966; Uchida, 1973; Van Iten et al., 2006; Werner, 1973). However, it is generally accepted that Staurozoa is the earliest diverging clade (Dawson, 2004). As living medusozoans are characterized fundamentally by tetraradiate symmetry, some zoologists believed that their common ancestor was most likely a sessile tetra-radial organism (Thiel, 1966; Werner, 1972). There are abundant discoid fossils from the Ediacara fauna displaying various symmetrical patterns, but they lack sufficient diagnostic medusozoan morphology (Young and Hagadorn, 2010; Yuan et al., 2011). To date, the oldest-known unequivocal crown-group medusae with four-fold symmetry came from the

Burgess-Shale type deposit of Cambrian Series 3 in Utah, USA (Cartwright et al., 2007).

The paucity of diagnostic characteristics in fossil medusozoans was fundamentally changed since the finding of exceptionally preserved phosphatized microscopic fossil embryos from the Cambrian Kuanchuanpu Formation in southern China. Especially those pentamerous fossils, *Punctatus* or *Olivooides*, are so impressive that they had attracted great attention of paleontologists owing to their early age, Orsten-type preservation in three dimensions, and intriguing biological affinity (Bengtson and Yue, 1997; Chen, 2004; Dong, 2009; Han et al., 2013; Steiner et al., 2014; Yao et al., 2011). X-ray micro computed tomography (Micro-CT) analysis revealed that some athecate pentamerous fossils may be ancestral cubozoans based on their delicate, exceptional internal anatomical structures such as interradial pairs of tentacles, gonad-lamellae, accessory lamellae, perradial frenula and velarial canals, etc. (Han et al., 2013) (Fig. 1F). However, this finding triggered many questions, i.e: are there any tetraradial cubzoans or medusozoans? What's the phylogenetic relationships between the pentaradial and tetraradial forms? Which symmetrical forms has more advantages in early Cambrian marine community? What are the preferred habit and habitat for pentamerous forms? etc. Indeed, there are some co-occurring tetraradial forms, including *Carinachites spinatus* (Qian, 1977), *Quadrapyrgites ningqiangensis* Li, 2007 (Li et al., 2007b), and an unnamed embryo with four oral lobes (Steiner et al., 2014). Although being accepted within a

5

framework of medusozoans, their systematic affinity remained ambiguous for the lacking of soft-tissue (Steiner et al., 2014; Steiner et al., 2004; Chen and Dong, 2008; Conway Morris and Chen, 1989; Li et al., 2007b; Qian, 1977; He, 1987). These tetraradial forms are so rare that they were supposed as an ecologically suppressed group in the shadow of pentamerous forms in the Cambrian marine community in South China. Here we describe three exceptionally-preserved specimens (ELISN83-66, 31-31, 131-38) of tetraradial cubozoans from the Kuanchuanpu Formation that will shed new light on the evolution of symmetric patterns of medusozoans.

3. Materials and methods

Our specimens were collected from the Lower Cambrian Kuanchuanpu Formation at the Shizhonggou section, Ningqiang County, Shaanxi, China. Fossils were recovered by dissolution of limestone in a 10% acetic acid. The specimen ELISN83-66 was analyzed using Synchrotron radiation X-ray tomographic microscopy (SRXTM) at SPring-8 in Hyogo, Japan (Append. 3S1-3). The Micro-CT data of specimens ELISN31-31 (Append. 3S4-6) and ELISN131-38 (Append. 3S7-9) were acquired at Tohoku University. All of them were photographed using the program VG Studio 2.2. 3D-rendering of various anatomical structures by different colors were created with VG Studio 2.2 Max. All specimens are deposited at the Early Life Institute, Northwest University, China. A cladistic analysis containing 25 taxa and 104 characters was analyzed in both PAUP* 4.0 b10 (Swofford, 2002) and TNT 1.1 (Goloboff et al.,

6

2008).

4. Preservation

Paleontologists now have attained a better understanding of the preservation of phosphatized microfossils from the Ediacaran-Cambrian sediments in South China (Komiya et al., 2008; Xiao et al., 2000). These microfossils had been subjected to microbial decay, transportation, secondary infilling, replacement, coating and reworking of other diagenesis (Steiner et al., 2014). Thus, most fossil eggs and embryos are dominated inside by the diagenetic structures, which sometimes has been mis-interpreted as biological anatomy. For example, the presumed 'egg-yolks' in these pentamerous embryos (Han et al., 2013; Yao et al., 2011) should better be explained as later void-fillings (Dong et al., 2013). However, combined with taphonomic analysis, paleontologists begin to distinguish the genuine traits from the secondarily diagenetic structures in dealing with those extremely rare, but well-preserved radial symmetric cnidarian fossils on the basis of the structural repetition (Han et al., 2013; Han et al., 2010). It means that an original biological structure should occur several times in the same position along the symmetrical axis in the same specimen, and that structure should be further confirmed by other specimens of same species or close related taxa.

Diagenesis of phosphatized microfossils is traditionally revealed in petrology by thin-section observations (Komiya et al., 2008), now it is also recognizable under

SRXTM or micro-CT examination (Dong et al., 2013; Yin et al., 2014). Based on micro-CT images of these cnidarian fossils, we recognized three different X-ray attenuation phases of phosphate, i.e., the whitish, grayish, and blackish phases, respectively. The variations in color from white to black might depend on the chemical composition, probably with the increasing CO_3^{2-} ions in phosphate (Komiya et al., 2008), but it need be further confirmed by chemical analysis combined with accurate micro-CT data. Apparently, minerals in the whitish phase (Figs. 2-6) are composed of cryptocrystalline apatite that had occasionally replicated the original biological tissues, including external and internal tissues as well as decayed organic substances; the latter, usually represented as filamentous microbes inside the fossils (Yue and Bengtson, 1989), had been accurately replicated at the earliest rapid phospatization (Steiner et al., 2014). The phosphatized tissues, sometimes have secondary coatings of acicular microcrystallites of apatite, which also lead to complete or partial void-fillings of the original cavities in the fossils, as seen in specimens ELISN66-15 (Han et al., 2013), ELISN131-38, and the manubrium in specimen ELISN31-31. The grayish minerals, mostly low-density phosphate with much more CO_3^{2-} content, infilling the voids constructed by the apatite (Figs. 2, 6), and were likely deposited lastly during later diagenetic mineralization. Seen from the specimen ELISN83-66 (Fig. 2I), the increasing CO_3^{2-} content is the chief "troublemaker" that had nibbled on primary cryptocrystalline phosphates leading to the serious loss of original biological information. The space defined by the blackish

8

mineral phase usually represents the remains of original body lumen and the residual space of bacteria-consumed tissues, as seen in specimen ELISN31-31 and other pentamerous cubozoans (Han et al., 2013).

5. Results

5.1 External anatomy

The three tetra-fold specimens (ELISN83-66, 31-31, 131-38) vary in shape and size. The spheroid specimen ELISN83-66, a peri-hatched individual *ca.* 600 μm wide, is divisible into a low quadrate pyramidal aboral end, a slightly swelling cylindrical median portion, and a constricted oral end that is strikingly delimited from other parts by a coronal groove (cg). The bell rim bears four equal-distanced larger and robust apertural lappets, which are intercalated with four pairs of smaller secondary lappets; all these axipetal lappets display a thickened rim (Figs. 1ADG, and 2T, 4L, 6L,7A), a pattern identical to those of co-occurring pentaradial forms (Fig. 1F) (Han et al., 2013). Undoubtedly those four principal lappets can precisely define the perradii (marked with "*" in Figs. 2-8) of the medusae (Haeckel et al., 1882; Han et al., 2013). The pyramidal aboral part is also distinct from the median part by four conspicuous longitudinal interradial furrows (marked with arrows). The interradial furrows extend oral-ward from the apex, firstly meet the subapical circumferential groove (scg), then plough across the median circumferential groove (mcg) of the median part (Fig. 1C), and finally reach the coronal groove (Fig. 1C; Figs. 2B-G).

The bell of the specimen ELISN31-31, *ca.* 400 μm wide, is highly impressive, resembling a minute pyramidal jar (Fig. 1DE). Its aboral part is separated from the oral ends by a middle part, which is also delimited by a lower conspicuous coronal groove and an upper vague subapical circumferential groove (Figs 4AB, 5A, C). ELISN31-31 differs from ELISN83-66 in that the former bears a strongly depressed subumbrella (Fig. 5B), four comparatively smaller perradial apertural lappets (pal) and eight inconspicuous adradial apertural lappets (aal) (Fig. 5A). Externally, the aboral end of ELISN31-31 shows four wide prominent interradial ridges intercalated with four inconspicuous perradial furrows (Fig. 5C). Either side of each interradial ridge exhibit two inconspicuous corner pillars (cp) (Figs. 1E, 4D).

The specimen ELISN131-38 exhibits no difference with ELISN83-66 in size and oral morphology. However, its incomplete aboral part is tapered greatly as a low pyramidal with four interradial furrows and four bulging perradial ridges. In addition, several protuberances peripheral to the apertural lappets (Figs. 1GH, 6K, 7A) are reminiscent of rhopalia in living medusae. But these protuberances are not strictly distributed in the same level at the perradii as rhopalia of existing cubozoans (Hyman, 1940), and thus might be assumed as nematocyst warts seen in living *Carybdea branchi* (Gershwin and Gibbons, 2009) or mere taphonomic artifact.

As the pentamerous cubozoans described previously (Han et al., 2013), all these tetraradiate fossils absent a flexible cuticularized exoskeleton or peridermal integument as those in *Olivooides*.

5.2 The bell cavity and related structures

Besides revealing many aspects of the internal anatomy between exumbrella and subumbrella, analysis by using X-ray micro-CT also reveals some subumbrellar structures, such as tentacles, frenula, and a velarium in these three specimens, which are described as follows.

5.2.1 Manubrium and vascular cavity: The central primordial manubrium (mb), which is short and deeply rooted near the stomach floor, is three-fourth length of the bell height in ELISN31-31 (Fig. 5B). A long esophagus (es) of the manubrium leads aborally to a small central stomach cavity (csc) (Figs. 4AE). A broad central stomach cavity is distinguished from the esophagus by a conspicuous internal constriction in ELISN131-38, the constriction here is interpretable as the pyloric opening (po) (Figs. 6AB, 7B). The manubrium in ELISN131-38 is octagonal cone-shaped, protrudes above the level of apertural lappets. The manubrium is seemingly fixed to the subumbrella by four suspensoria (sp) in the perradii (Fig. 6F). The mouth of the manubrium remains closed in both specimens. In ELISN83-66, the manubrium is almost completely missing (Figs. 2F, 3C) and the central stomach cavity is entirely filled with secondary low-density phosphate. Peripheral to the central stomach cavity, the other vascular cavities among the three fossils also vary in space, which are much broader in ELISN83-66 (Fig. 3C) and ELISN131-38 than that in ELISN31-31.

11

5.2.2 Velarium and frenulum: An annular velarium, which is more evident in ELISN83-66 than both ELISN 131-38 and ELISN31-31, is suspended by a ring of twelve prominent vertical bracket-like ridges on the subumbrellar wall. The ridges are interpreted as four principal perradial frenula (pfr) intercalated with four pairs of small adradial frenula (afr) (Figs. 2C, 3A, 4K, 5A, 6H, 7A, 3DE) as in known pentamerous cubozoans (Han et al., 2013). These frenula are well congruent in disposition with underlying apertual lappets as in pentamerous cubozoans (Han et al., 2013). In ELISN31-31, three short, tiny diverticula visible at the adaxial distal end of each perradial frenulum are interpretable as the velarial canals (vc) (Figs. 4K, 5D). The velarial canals are respectively continuous with two lateral margins and a central prominent radial ridge of the apertural lappets (Fig. 5A, D). Its three-dimensional configuration is apparently stouter than those of sheet-like ones in mechanics.

5.2.3 Coronal muscles: A sheet of fine striated concentric coronal muscles (crm) along the subumbrella margin of ELISN83-66 is clearly interrupted at each interradius (Figs. 1B, 2AB, ST, 3ABD). Notably at the perradii, these coronal muscles within the velarium extend but turn nearly 90 degrees in a horizontal and radial orientation into the primary and secondary frenula; some of these muscles in frenula run back to the lower subumbrella (Figs. 2ST). Thus the velarial muscles are continuous with the inferred frenular musculature. Another sheet of striated concentric and curved muscles is also present in perradial apertural lappets. However, they are restricted at the exumbrella margin and are separated from the velarial and frenular muscles by a

12

ring canal (Fig. 2T). Thus, both the exumbrella and subumbrella possess striated muscles. Those coronal muscles are commonly seen in the subumbrellar margin of living coronates ((Russell, 1970), Text-Figs. 58, 68) and the cubomedusans such as *Tripedalia cystophora* (Satterlie et al., 2005). On contrast, each fossil muscle fiber (*ca.* 10 μm in diameter) is less but much stouter than that in recent forms (less than 5 μm). Besides of interradii, the coronal muscles in ELISN83-66 are likely interrupted at each perradius as extant cubozoans (see Figs. 8CD).

5.2.4 Interradial septa: The external interradial furrows on the exumbrella usually indicate the locations of the interradial septa (Figs. 2BC, 6C-H). In ELISN83-66, the interradial septa are not simple plate-like, but appearing as fused conjunction points riveting the exumbrella and subumbrella at each interradius (Figs. 2DE, 3F). In cross sections, the interradial septa in ELISN131-38 appear as four triangular interradial septal ridges (isr) at the middle portion of the bell (Figs. 6EGI; 7CE). Due to the riveting of four interradial septa, the exumbrella and subumbrella in above specimens stand close to each other at the interradii, and as a result shaping the bell into four scalloped sections. In ELISN31-31, the ex- and sub-umbrella walls are additionally connected by the perradial septa (ps) (Figs. 4EG), and the latter is termed here referring to the perradial fusion of exumbrella and subumbrella. At the apical part of the specimen, the interradial septa are long nail-like in cross sections (Figs. 4CD) and are connected to a rather small central stomach cavity (csc) that is restricted near the bell apex (Figs. 4AC).

5.2.5 Claustra*:* Adjacent interradial septa in these three specimens are bridged by four thin vertical plates of claustra (cl), which extend orally and are continuous with the endoderm of the subumbrella (Figs. 2DH, 4DG, 6EF). Besides central stomach cavity (Figs. 7BF), such coalescences partition the body cavity into an inner subumbrellar cavity and four peripheral perradial pockets. These vascular cavities vary greatly in size from each other. Nevertheless, there are other internal anatomical structures varying remarkably among these three specimens.

5.2.6 Gonad-lamellae and middle funnel*:* Four pairs of longitudinal lamellae, which are derived from the exumbrellar wall, are visible at either side of each interradial septum near the apical part of the medusae; these lamellae are tentatively interpreted as the gonad-lamellae (gl) (Fig. 4E). More orally in ELISN83-66 and ELISN131-38, the lateral extension and fusion of two adjacent gonad-lamellae in the same perradial pocket constitute a longitudinal median funnel (mf) in-between the subumbrella and exumbrella (Figs. 2E, 3BC, 6F-I, 7BC). The middle funnels in both specimens run downward to the bell margin and are eventually fused with polygonal subumbrella near the horizontal level of the coronal groove (Figs. 2G-N, 6C-H). The middle funnels in ELISN131-38 are rather vague, but are recognizable as four dark slits in cross section, and they are fixed to the exumbrella by the interradial septa (Figs. 6C-H, 7BC). In ELISN83-66, the middle funnels are evidently united to the exumbrella by interradial septa and perradial septa (Figs. 2I-P). More oral-ward, they are additionally

connected to the subumbrella by four secondary suspensoria (ssp) in the perradii (Figs. 2I-P).

The putative gonad-lamellae in specimen ELISN31-31 are quite different from the above two specimens. They are rather short but directly support the subumbrella together with the interradial septa and perradial septa, thus imparting the subumbrella near the apical part an appearance of four-petal shape in cross section and displaying diagnostic four interradial subumbrellar ridges (isur) (Figs. 4D-G). Additionally, eight short adradial marginal lamellae (aml) arise from the inner side of the exumbrellar wall (Figs. 8FG), well corresponding to the external corner pillars. These marginal lamellae are quite close to the exumbrellar wall, each bridging the exumbrellar bases of both accessory septa and adjacent perradial septa.

5.2.7 Tentacles: In the light of co-occurring pentamerous cubozoans (Fig. 5E) (Han et al., 2013), four pairs of interradial tentacle buds, although poor in preservation in these three specimens, are discernible by either a few of remains within the subumbrellar cavity (Figs. 2AN-P, 3E, 6J) or their short thread-like tentacular roots fixing to the exumbrella (Fig. 2AN-P, 4AIJ, 6J). Notably, in ELISN31-31, each interradial pair of tentacular remains, which are well separated from each other by the interradial septa, are rooted respectively at the adradii of the exumbrellar wall, thus being quite close to adjacent corner pillars (Figs. 4IJ, 5B, D, 8A). In contrast, both tentacles of each interradial pair are connected to the same interradial septum in

pentamerous cubozoan fossils (Han et al., 2013) (Fig. 8B). These septal roots probably represent longitudinal muscles.

5.2.8 Ring canal: A ring canal (rc) is visible between two body walls along the bell margin (Figs. 2BQ-T, 4AB K, 6A), it is located peripheral to the coronal muscles in ELISN83-66.

5.2.9 Umbrella thickness: As evident in cross sections, the exumbrella is much thicker than subumbrella in the specimen ELISN31-31 (Figs. 8A-B, 5B, D) and extant cubozoans (Conant, 1898). However, such distinction is not so evident in other tetraradial (Figs. 2-6, 8F-G) and pentaradial Kuanchuanpu medusozoans (Han et al., 2013) as well as existing staurozoans (Uchida, 1929). On the contrary, both ELISN108-343 and GMPKU3089 have a much thicker subumbrellar wall. It appears that such a body-wall differentiation in thickness represents most probably an original configuration rather than a taphonomic bias of secondary coating. The significance of the body-wall differentiation in functional morphology is unknown. However, thick umbrella wall in medusa usually indicates thick mesoglea, which have a variety of functions, including maintenance of buoyancy and as a skeleton for elastic recoil following the muscular contraction (Arai,1997).

6. Discussions

6.1 Zoological affinity

One body opening is one of the compelling characteristics to distinguish

16

diploblastic cnidarians from triploblastic eubilaterians. X-ray micro-CT analysis confirmed that the broad opening (equivalent to velarial opening) of concaved subumbrellar cavity in the referred fossils is blind toward the aboral side; the real unique mouth is located at the free end of the central stalk-like manubrium. The closed state of the mouth opening in these fossils can be justifiably interpreted as most likely owing to their peri-hatched developmental status. Therefore, no trace of a through gut (thought mouth to anus) as in triploblastic animals occurs in the current tetraradial fossils. Extant and Cambrian ctenophores (Conway Morris and Collins, 1996; Hu et al., 2007; Hyman, 1940), which resemble cnidarians in their radial symmetry, have a central body opening at the oral side but lack a manubrium within the "U"-shaped subumbrellar cavity. In addition, regardless of the apical statocysts at the aboral end of ctenophores, the aggregation of subumbrellar tentacles and the lack of comb plates in the tetraradial fossils are inconsistent with fossil and extant ctenophores. Thus, the discussion of their affinity should be restricted within the framework of cnidarians (Dong et al., 2013; Liu et al., 2014; Van Iten et al., 2010; Van Iten et al., 2014). The tetraradial symmetry, marginal lappets, and concentration of tentacles in the interradii are absent in bilateral anthozoans.

Within a framework of medusozoans, hydrozoans and staurozoans can be confidently excluded in current considerations. The hydrozoans are characterized by a velum but devoid of any frenula; the concentration of tentacles and gonads, if present, are located at the perradial. The developments of middle funnels between subumbrella

17

and exumbrella are also unlikely for hydrozoans because their body walls are almost completely fused except for the radial canals (Hyman, 1940). Even if the potential of sessile habit for those tetraradial fossils cannot be completely excluded, the presence of apertural lappets, frenula, moderately partitioning of the gastric cavity, and the lack of groups of secondary tentacles on adradial arms disfavor their phylogenetic placement within staurozoans.

Although still not conclusive (Kayal et al., 2013), most scientists agree that extant cubozoans and scyphozoans are sister groups (Collins et al., 2006). They share many traits such as paired gonads and strong coronal muscles. It has been proposed that Kuanchuanpu medusozoans, especially those with external periderms, are related to scyphozoans, especially coronates (Dong et al., 2013; Liu et al., 2014; Van Iten et al., 2014). However, the disposition of the tentacles and the lack of adradial lappet nodes in these tetramerous fossils are incompatible with those of scyphozoans. In contrast, the configurations of the tentacles, apertural lappets and frenula in current fossils are highly comparable with co-occurring pentaradiate cubozoans previously suggested (Han et al., 2013). A set of shared traits among these pentaradial and tetraradial fossils, such as the aggregation of subumbrellar pairs of short tentacles in the interradial, and a velarium suspended by frenula, suggesting that current tetraradial forms as well as those pentamerous fossils belong to a new monophyletic stem group of Cubomedusae instead of a crown group.

6.2 Phylogeny of Kuanchuanpu medusozoans

We carried out a preliminary cladistic analysis based on 25 taxa and 104 characters in PAUP* 4.0 b10 (Append. 1) and TNT 1.1 (Append. 2). The data matrix derives in large part from the refs (Marques and Collins, 2004; Van Iten et al., 2006) by supplementing new data from Kuanchuanpu medusozoans. The proposed fossils of Cubozoa, Coronate, Semaeostomae and Narcomedusae (referred respectively as 'cormr', 'cubomr', 'narmr', 'semamr' in Figure 9 and Appends. 1-2) from the Middle Cambrian Marjum Formation (Cartwright et al., 2007) were listed into the new character matrix together with Kuanchuanpu medusozoans. All 104 characters have equal weight, 8 of them are constant, 26 variable characters are parsimony-uninformative, and the rest 70 characters are parsimony-informative. The unweighted analysis of the data matrix in PAUP analysis yielded 2628 trees (Tree length (TL)=184, Consistency index (CI)=0.6250, Rescaled consistency index (RC)=0.4732). The successive weighting analysis (Marques and Collins, 2004; Van iten, et al., 2006) resulted in three trees (TL=95.86191, CI=0.8415, RC=0.7494) that differing in the position of Conulariids (Append. 1). In TNT analysis, we got 100 trees by Implicit enumeration search. The first (Append. 2A) and the consensus trees (Append. 2B) are generally concordant with that of PAUP, and the common synapomorphies of 100 trees are mapped on the first tree (Append. 2A).

Our cladistic hypothesis (Fig. 9) is largely congruent with previous medusozoan phylogeny. Although the Hydromedusae is found allying with Scyphomedusae, it is weakly supported by Bootstrap analysis (Append. 1). Particularly, a monophyletic

group constituted by Kuanchuanpu medusozoans is well supported sister to extant and Middle Cambrian Cubomedusae in Bootstrap analysis (Append. 1). The results of such analyses, especially class-level relationships, however, must be regarded as indicative rather than definitive on account of incomplete fossil preservation that leading to a high percentage of missing data and parsimony-uninformative data, as well as the uncertainties of interpretation (Briggs and Bartels, 2010).

6.3 Characteristic analysis

6.3.1 Tentacles: Because in living medusozoans, the interradial tentacles and perradial tentacles (usually reduced as rhopalia) are generally considered as primary tentacles, they are respectively considered as homologues and occur ontogenetically earlier than other tentacles (Thiel, 1966; Werner et al., 1971). For example, *Tripedalia xaymacana* (Tripedaliidae, Carybdeida, Cubozoa) has four perradial rhopalia and a group of three tentacles at each interradial corner, including a central plus two lateral ones; the canal of all tentacles is opened independently into the peripheral gastrovascular system. Undoubtedly, the central tentacle in each group is the homologue of the single tentacle of other species of Carybdeidae, Alatinidae, and Tamoyidae. Because the central tentacle arises earlier than two adjacent lateral tentacles (Conant, 1898), thus, it should be regarded as primary ones together with perradial rhopalia; whereas those lateral ones in Charybdea cubozoans are likely secondary. However, there is one exception, i.e. *Tripedalia binata* Moore 1988 possesses a pair of separated lateral tentacles on either side of each interradius, but

lacks interradial primary tentacles. The two lateral tentacles are most likely homologous with the corresponding tentacles of *Tripedalia xaymacana*.

All known tetraradial and pentaradial Kuanchuanpu cubozoans, although quite different from each other with regard to their internal anatomy, constitute a new monophyletic group based on the shared feature, *i.e.* a pair of subumbrellar tentacles distributed on either side of each interradial septum (character 101 in Fig. 9 and Appends. 1-2). These tentacles are highly analogous to those of *Tripedalia binata* in disposition, and thus should be considered homologous. However, *Tripedalia binata* differs from these fossils in many other aspects, particularly in four perradial rhopalia that are absent in current Kuanchuanpu cubozoans.

In addition, each paired tentacles are quite close in the known pentamerous Kuanchuanpu cubozoans because they share the same septal root fixed on the interradial septum (Fig. 8E). In contrast, the paired tentacles are well distanced in ELISN31-31 because each tentacle seemingly has independent septal roots away from the interradial septa (Fig. 8F). More accurately, these tentacles are located at the adradii. Such disposition is reminiscent of short capitate secondary tentacles of staurozoans, especially in *Thaumatoscyphus distinctus* Kishinouye (Uchida and Hanaoka, 1933) with short arms. Probably all these secondary tentacles aforementioned in extant staurozoans, cubozoans, and fossil cubozoans are homologous. If this is the case, the comparatively short tentacles of these Kuanchuanpu cubozoans, which mostly remain in peri-hatched condition, are likely

21

homologous with those of short secondary tentacles in staurozoans.

Furthermore, as previously proposed (Han et al., 2013), tentacles restricted deep within subumbrellar cavity represent a primitive condition for cubozoans in contrast with those of extant forms extending outside the velarium as the development of pedalia (see Fig. 8C-D). The subumbrellar tentacles of some Kuanchuanpu cubozoans are located quite close to the bell rim (Han et al., 2013, fig. 2G-I), probably representing a derived feature commonly seen in extant medusozoans.

6.3.2 Endodermic perradial fusion and rhopalia: Compared with other extant medusozoan classes, the cubozoans are highly specialized as sensory organs (rhopalia) with elaborate complex eyes and statocysts. The rhopalia are ontogenetically transformed from the subumbrellar perradial tentacles (Conant, 1898; Thiel, 1966). Particularly at the perradii, the endodermis of subumbrella and exumbrellar walls are longitudinally fused ranging from the sensory niches downward to the bell margin, and the fusion partitions each perradial pocket into two small marginal pockets but where in-between leaves a radial canal of rhopalia (rcr) (Fig. 8B) (Conant, 1898). Unfortunately, as mentioned above, neither rhopalia nor short sensory stalks can be found in the perradii of co-occurring pentamerous fossil cubozoans (Han et al., 2013). That absence was previously inferred to be possibly related either to their embryonic status or to taphonomic artifacts (Han et al., 2013). However, the rhopalia, one of the typical features seen in extant scyphomedusans and cubomedusans, are also absent in ephyra-like pentaradiate fossils (Dong et al., 2013, Fig. 4) and current tetraradial

forms. We suspected that these pentamerous fossils most likely lack rhopalia in their whole life.

The Kuanchuanpu cubozoans exhibit a variety of perradial fusion. In ELISN108-343, the ex- and subumbrellar walls keep far away from each other by spacious perradial pockets. The longitudinal fusion in their perradii, represented by the suspensoria and secondary suspensoria, occurs either between the exumbrella and other endodermic lamellae or between the subumbrella and other endodermic lamellae (Han et al., 2013). The perradial fusion in ELISN83-66, represented by perradial septa and secondary suspensoria (Figs. 4I-O), is analogous to those of pentamerous forms. In contrast with those above mentioned forms, ELISN31-31 displays a limited, but directed endodermic fusion as perradial septa between exumbrella and subumbrella, thus quite close to the situation in those of extant cubomedusae (Figs. 4G, 8F). Thus, we infer such an umbrella fusion, functionally serving for reinforcing the bell walls, had compressed the vascular space of sensory organs in extant cubomedusans.

As illustrated by ELISN31-31, the perradial septa, in combination with the corner pillars, contributes to further shaping the subquadrate profile of the cubomedusans (Fig. 4, Append. 3S4). Nevertheless, compared with a diversity of well-partitioned gastric pockets in pentaradiate cubozoans, the endodermic perradial fusion of exumbrella and subumbrella in extant forms and the fossil specimen ELISN31-31 inevitably leads to the reduction and narrowing of the lumens of gastric cavity but contrarily expands the space of the subumbrellar cavity. It is reasonable to

23

infer that large subumbrellar cavity could be much more efficient and adaptive in contractile swimming of cubomedusae at the aid of the strong coronal muscles and the velarium. Similarly in scyphomedusans and hydromedusans, the lappet nodes in the adradii, as well as radial canals should be extreme results of the endodermic fusion of exumbrella and subumbrella (Fig. 4 in (Thiel, 1966)). The endodermic fusion is not always being restricted at the perradii. Remarkably, stauromedusans, a lineage of sessile medusae that occupy the basal position of medusozoan phylogeny (Collins, 2009; Collins and Daly, 2005; Marques and Collins, 2004), possess broad but poorly-partitioned vascular cavities but lack such a kind of fusion. Thus in summary, the endodermic fusion, is proposed here not only as one of the important characteristics in the phylogeny of medusozoans, but also of great functional significant in sculpturing the external shape, and developing the pelagic life habit in different lineages of medusa.

6.3.3 Apertural lappets: To find the counterpart of apertural lappets in extant medusozoans is critical in understanding the classification and evolution of current Kuanchuanpu medusozoans. The perradial and adradial apertural lappets are respectively continuous with the perradial and adradial frenula in all known tetra- and penta- radial cubozoan fossils (Figs. 7D), this reveals that the apertural lappets are substantially supported by the frenula. In living cubomedusans, the circular velarium is supported by five perradial frenulae, this lead to the assumption that whether the circular velarium are derived from the discrete apertural lappets? Interestingly, the

24

velarium of the cubmedusans is commonly accounted to have arisen by fusion of discrete marginal lappets (or 'marginal lobes') (Constant, 1898), and such marginal lappets, triangular in shape, are visible at their very juvenile stage (see Han et al., 2013, fig. 1C). In the later stages, the marginal lappets will develop forked diverticula (Uchida, 1933, Fig. 63), which finally became the velarial canals of the velarium. Thus, it has been proposed that ancestral cubomedusans lacks a velarium but with many free marginal lappets (Constant, 1898). Fortunately, in ELISN31-31 we found the tiny diverticula at the distal end of each perradial frenulum, they are respectively continuous with two lateral margins and a central prominent radial ridge of the apertural lappets in ELISN31-31. If this is the case for adradial apertural lappets and adradial frenulae, thus, it is highly potentials that the apertural lappets, especially the adradial ones, are precursors of velarial canals of extant cubomedusans.

In addition, the perradial "apertural lappets" seen in *Malo filipina* Bentlage and Lewis, 2012 (Carukiidae, Carybdeida, Cubozoa) and *Morbakka virulenta* Kishinouye, 1910 (Bentlage and Lewis, 2012) (Tripedaliidae, Carybdeida, Cubozoa) are merely thickenings of the velarium (B. Bentlage, personal communication). It is still difficult to claim that they are homologous with large perradial lappets in Kuanchuanpu medusozoans. Both apertural lappets and frenula are never found in recent staurozoans, but the former are widely distributed in scyphozoans. It is not impossible that these structures have been acquired in the common ancestor of cubozoans and scyphozoans, but had been partly degenerated in different lineages of modern

medusozoans.

6.3.4 Corner pillar: The fossil cubozoans known remarkably differ from other extant medusozoans by their box-shaped bell with tentacles concentrating at the four interradial corners each with a pair of longitudinal ridge-like corner pillars (Fig. 8B). Exceptionally, such pillars occur merely in ELISN31-31 (Figs. 8FG), indicating that the condition of exumbrella in ELISN31-31 is much similar to modern crown-group cubozoans.

6.4 Evolution of tetraradial crown-group Cubomedusae

Living medusozoans, including cubomedusans, are dominated by tetraradial symmetry (Hyman, 1940), which is regarded as a symplesiomorphy during traditional phylogenetic analysis (Collins, et al., 2006; Marques and Collins, 2004; Thiel, 1966; Werner et al., 1971). The common ancestor of medusozoans was supposed to bear with four septa and four tentacles (Collins, et al., 2006). The current phylogenetic analysis (Fig. 9) appears congruent with the tetraradial hypothesis while the pentaradial symmetry be a derived feature. However, it is not inclusive due to the incompleteness of data matrix. Other symmetrical patterns have long been known to occur sporadically in populations of medusozoans, and some hydrozoans display a genetically fixed pentaradial symmetry (Uchida, 1928; Xu et al., 2014). Among early Cambrian medusozoan candidates, there are divergent symmetric types, which sometimes occur in a single lineage. For example: conulariids shows biradial symmetry (Van Iten et al., 2006); tetraradial symmetry occasionally co-occurs with

26

anabarites generally showing triradial symmetry (Kouchinsky et al., 2009; Kouchinsky et al., 1999; Yue and Bengtson, 1999); a few of triradial and pentaradial forms co-occur with tetraradiate carinarchitids (Liu et al., 2011).

The microanatomy of current cubozoan fossils gives a high-resolution support for the hypothesis that medusozoans are not restricted at the tetraradial symmetry (Han et al., 2013). These pentaradiate and tetraradiate fossils constitute a monophyletic group on the basis of a set of shared traits such as pairs of interradial tentacles and perradial and adradial apertural lappets and frenula. In this clade, those peridermal forms, including pentaradial *Punctatus* and tetraradial *Quadrapyrgites*, constitute the family olivooidae (Li et al., 2007b; Steiner et al., 2014) (Fig. 9). In addition, concerning the development of perradial fusion and corner pillar among current tetraradial forms, ELISN83-66 and ELISN131-38 are closer to those known pentamerous forms whereas ELISN31-31 resembles extant crown-group cubomedusans (Fig. 9). We can hypothesis that (1), different symmetric patterns had been independently acquired in different lineages (Fig. 10); (2) the symmetric patterns could not be emphasized as a high-level classification criterion for Cambrian medusozoans; (3) it is still immature to confirm which symmetric pattern represents symplesiomorphy of medusozoans.

We knew that the earliest crown-group cubozoans and scyphozoans appeared in the Cambrian Stage 5 (Cartwright et al., 2007). However, the crown group should predate the Cambrian Stage 3 due to the appearance of eubilaterians especially their crown-groups (Chen, 2004; Han et al., 2004) concerning the phylogenetic trees of

metazoans. The expected crown-group cubomedusans might have been evolved during the first two stages of Cambrian, like ELISN 31-31.

The prevalence of pentaradial symmetry and the divergence of other symmetric patterns in Kuanchuanpu medusozoans are still unknown. But it appears that the tetramerous forms might have gradually escaped from the shadow of pentamerous and other symmetric competitors, and had finally acquired their ecologically dominance probably around middle early Cambrian. What are the substantial advantages behind the dominance of tetraradial forms for cubozoans and other medusozoans in the geohistory succeeding the Fortunian Stage still remain obscure. Different symmetry for medusozoans means a different amount of tentacles, septa, gastric pockets and other associated organs. The cryptic symmetric advantages for all major lineages of medusozoans should be significant as the occurrence of triploblastic bilaterians and stepwise establishment of modern-type ecosystem in the first three stages of the early Cambrian (Vannier et al., 2007; Zhang et al., 2014).

7. Conclusions

The Cambrian Kuanchuanpu fauna include a divergent of pentamerous and tetramerous medusae; these fossils, similar in external morphology, but strikingly differs from each other in their internal anatomical structures. They most probably represent essentially quite different genus-level taxa. Cladistic analysis implies that they constitute a robust monophyletic clade of medusozoans because of the shared traits of perradial frenula and the interradial concentration of subumbrellar tentacles.

28

However, a series of features, including the presence of apertural lappets and adradial frenula, the lack of both interradial primary tentacles and rhopalia, can sufficiently distinguish them from extant cubomedusans and support a stem-group assignment. Given various symmetrical patterns occurred among different lineages of Cambrian cubozoans and other medusozoans candidates, the search of the common ancestor of medusozoans should not be restricted at the tetraradial forms.

8. Abbreviations

The morphological terminology mainly follows the ref (Han et al., 2013). aal, adradial apertural lappets (blue violet); afr, adradial frenulum (grass green); aml, adradial marginal lamellae; bc, bell cavity (subumbrellar cavity); cg, coronal groove; cl, claustrum; cp, corner pillar; crm, coronal muscles (dark green); csc, central stomach cavity; en, egg envelope (claybank); es, esophagus; eu, exumbrella (orange); g, gonad; gl, gonad-lamella (light purple); go, gastric ostium; if, interradial furrow; ir, interradial ridges; is, interradial septa (blue); isr, interradial septal ridge; isur, interradial subumbrellar ridges; mb, manubrium (orchid pink); mcg, middle circumferential groove; mf, middle funnel; mp, marginal pocket; n, nerve; pal, perradial apertural lappet (dark blue); pd, pedalia; pf, perradial furrow; pfr, perradial frenulum (turquoise); po, pyloric opening; pp, perradial pocket; ps, perradial septum; pt, protuberance; rc, radial canal; rcr, radial canal of rhopalia; rh, rhopaloid; rr, radial ridge; sal, secondary apertural lappet; scg, subapical circumferential groove; sf, septal funnel (grass green); sfr, secondary frenulum; srt, septal root of tentacles; su,

29

subumbrella (brown); suc, subumbrella cavity; sp, suspensorium; sn, sensory niche; ssp, secondary suspensorium; tb, tentacular bud (grey); ve, velarium (sky blue); vc, valarial canal; vlm, vertical lamella of bell margin; *, perradius; →, interradius; +, adradius.

10. Acknowledgments

11. References

Arai M.N. 1997. A Functional Biology of Scyphozoa. London: Chapman & Hall.

Bengtson, S., Yue, Z., 1997. Fossilized metazoan embryos from the earliest Cambrian. Science 277, 1645-1648.

Bentlage, B., Lewis, C., 2012. An illustrated key and synopsis of the families and genera of carybdeid box jellyfishes (Cnidaria: Cubozoa: Carybdeida), with emphasis on the "Irukandji family" (Carukiidae). Journal of Natural History 46, 2595-2620.

Briggs, D.E., Bartels, C., 2010. Annelids from the Lower Devonian Hunsrueck Slate (lower Emsian, Rhenish Massif, Germany). Palaeontology 53, 215-232.

Cartwright, P., Halgedahl, S., Hendricks, J., Jarrard, R., Marques, A., Collins, A., Lieberman, B., 2007. Exceptionally preserved jellyfishes from the Middle Cambrian. PLoS One 2, e1121.

Chen, F., Dong, X.P., 2008. The internal structure of Early Cambrian fossil embryo *Olivooides* revealed in the light of Synchrotron X-ray Tomographic Microscopy. Chinese Science Bulletin 53, 3860-3865.

Chen, J.Y., 2004. The Dawn of Animal World. Jiangsu Science and Technology Press, Nanjing.

Collins, A.G., 2002. Phylogeny of Medusozoa and the evolution of cnidarian life cycles. Journal of Evolutionary Biology 15, 418-432.

Collins, A.G., 2009. Recent insights into cnidarian phylogeny. Smithsonian Contributions to the Marine Science 38, 139-149.

Collins, A.G., Daly, M., 2005. A new deepwater species of Stauromedusae, *Lucernaria janetae* (Cnidaria, Staurozoa, Lucernariidae), and a preliminary investigation of stauromedusan phylogeny based on nuclear and mitochondrial rDNA data. Biological Bulletin 208, 221-230.

Collins, A.G., Schuchert, P., Marques, A.C., Jankowski, T., Medina, M., Schierwater, B., 2006. Medusozoan phylogeny and character evolution clarified by new large and small subunit rDNA data and an assessment of the utility of phylogenetic mixture models. Systematic Biology 55, 97-115.

Conant, F.S., 1898. The Cubomedusæ: a memorial volume. The Johns Hopkins Press, Baltimore.

Conway Morris, S., Chen, M.E., 1989. Lower Cambrian anabaritids from south China. Geological Magazine 126, 615-632.

Conway Morris, S., Collins, D., 1996. Middle Cambrian ctenophores from the Stephen Formation, British Columbia, Canada. Philosophical Transactions: Biological Sciences, 279-308.

Dawson, M., 2004. Some implications of molecular phylogenetics for understanding biodiversity in jellyfishes, with emphasis on Scyphozoa. Hydrobiologia 530, 249-260.

Dong, X.P., 2009. The anatomy, affinity and developmental sequences of Cambrian fossil embryos. Acta Palaeontologica Sinica 48, 390-401.

Dong, X.P., Cunningham, J.A., Bengtson, S., Thomas, C.W., Liu, J.B., Stampanoni, M., Donoghue, P.C.J., 2013. Embryos, polyps and medusae of the Early Cambrian scyphozoan *Olivooides*. Proceedings of the Royal Society B-Biological Sciences 280.

Gershwin, L.A., Gibbons, M.J., 2009. *Carybdea branchi*, sp. nov., a new box jellyfish (Cnidaria: Cubozoa) from South Africa. Zootaxa 2088, 41-50.

Goloboff, P.A., Farris, J.S., Nixon, K.C., 2008. TNT, a free program for phylogenetic analysis. Cladistics 24, 774-786.

Haeckel, E., Murray, J., Thomson, C.W., 1882. Report on the deep-sea medusae dredged by HMS Challenger during the years 1873-1876. Hodges, Figgis, & Company.

Han, J., Kubota, S., Li, G., Yao, X., Yang, X., Shu, D., Li, Y., Kinoshita, S., Sasaki, O., Komiya, T., Yan, G., Yasui, K., 2013. Early Cambrian pentamerous cubozoan embryos from South China. PLoS One 8, e70741.

Han, J., Kubota, S., Uchida, H., Stanley Jr, G.D., Yao, X., Shu, D., Li, Y., Yasui, K., Lalueza-Fox, C., 2010. Tiny Sea Anemone from the Lower Cambrian of China. PLoS One 5, e13276.

Han, J., Shu, D., Zhang, Z., Liu, J., 2004. The earliest-known ancestors of Recent Priapulomorpha from the Early Cambrian Chengjiang Lagerstätte. Chinese Science Bulletin 49, 1860-1868.

He, T.G., 1987. Early Cambrian conulariids from the Yangtze platform and their early evolution Journal of Chengdu College of Geology 14, 7-18 (in Chinese with English Summary).

Hu, S., Steiner, M., Zhu, M., Erdtmann, B.D., Luo, H., Chen, L., Weber, B., 2007. Diverse pelagic predators from the Chengjiang Lagerstätte and the establishment of modern-style pelagic ecosystems in the early Cambrian. Palaeogeography, Palaeoclimatology, Palaeoecology 254, 307-316.

Hyman, L.H., 1940. The Invertebrates. McGraw Hill, New York.

Kayal, E., Roure, B., Philippe, H., Collins, A.G., Lavrov, D.V., 2013. Cnidarian phylogenetic relationships as revealed by mitogenomics. Bmc Evolutionary Biology 13, 5.

Komiya, T., Suga, A., Ohno, T., Han, J., Guo, J.F., Yamamoto, S., Hirata, T., Li, Y., 2008. Ca isotopic compositions of dolomite, phosphorite and the oldest animal embryo fossils from the Neoproterozoic in Weng'an, South China. Gondwana Research 14, 209-218.

Kouchinsky, A., Bengtson, S., Feng, W., Kutygin, R., Val'kov, A., 2009. The Lower Cambrian fossil Anabaritids: affinities, occurrences and systematics. Journal of Systematic Palaeontology 7, 241-298.

33

Kouchinsky, A., Bengtson, S., Gershwin, L., 1999. Cnidarian-like embryos associated with the first shelly fossils in Siberia. Geology 27, 609-612.

Li, G.X., Steiner, Zhu, M.Y., Yang, A.H., Wang, H.F., Erdtmann, B.D., 2007a. Early Cambrian metazoan fossil record of South China: Generic diversity and radiation patterns. Palaeogeography, Palaeoclimatology, Palaeoecology 254, 229-249.

Li, P., Hua, H., Zhang, L.Y., Zhang, D.D., Jin, X.B., Liu, Z., 2007b. Lower Cambrian phosphatized *Punctatus* from southern Shaanxi and their ontogeny sequence. Chinese Science Bulletin 52, 2820-2828.

Liu, Y.H., Li, Y., Shao, T.Q., Zheng, X., Zheng, J., Wang, G., Wang, H.Q., Wang, K., 2011. A new genus and specie of protoconulariids from the early Cambrian in the south Shaanxi, China. Acta Micropalaeontologica Sinica 28, 245-249 (in Chinese with English Summary).

Liu, Y.H., Li, Y., Shao, T.Q., Zhang, H.Q., Wang, Q., Qiao, J.P., 2014. *Quadrapyrgites* from the lower Cambrian of South China: growth pattern, post-embryonic development, and affinity. Chinese Science Bulletin 59, 4086-4095.

Maloof, A.C., Porter, S.M., Moore, J.L., Dudás, F.Ö., Bowring, S.A., Higgins, J.A., Fike, D.A., Eddy, M.P., 2010. The earliest Cambrian record of animals and ocean geochemical change. Geological Society of America Bulletin 122, 1731-1774.

Marques, A.C., Collins, A.G., 2004. Cladistic analysis of Medusozoa and cnidarian evolution. Invertebrate Biology 123, 23-42.

Qian, Y., 1977. Hyolitha and some problematica from the Lower Cambrian Meishucun Stage in central and SW China. Acta Palaeontologica Sinica 16, 255-275 (in Chinese with English Summary).

Russell, F.S., 1970. The Medusae of the British Isles: 2. Pelagic Scyphozoa with a supplement to the first volume on Hydromedusae.

34

Satterlie, R.A., Thomas, K.S., Gray, G.C., 2005. Muscle organization of the cubozoan jellyfish *Tripedalia cystophora* Conant 1897. The Biological Bulletin 209, 154-163.

Shu, D., Isozaki, Y., Zhang, X., Han, J., Maruyama, S., 2014. Birth and early evolution of metazoans. Gondwana Research 25, 884-895.

Steiner, M., Qian, Y., Li, G., Hagadorn, J.W., Zhu, M., 2014. The developmental cycles of early Cambrian Olivooidae fam. nov. (?Cycloneuralia) from the Yangtze Platform (China). Palaeogeography, Palaeoclimatology, Palaeoecology 398, 97-124.

Steiner, M., Zhu, M.Y., Li, G.X., Qian, Y., Erdtmann, B.D., 2004. New early Cambrian bilaterian embryos and larvae from China. Geology 32, 833-836.

Swofford, D.L., 2002. PAUP*. Phylogenetic analysis using parsimony (* and other methods). Version 4. Sunderland, Massachusetts: Sinauer Associates.

Thiel, H., 1966. The evolution of Scyphozoa: A review. The Cnidaria and their evolution. Academic, London, 77–117.

Tinggui, H., 1987. Early Cambrian conulariids from Yangtze platform and their early evolution. Journal of Chengdu University of Technology (Science & Technology Edition) 14, 7-18.

Uchida, T., 1928. Short notes on medusae. 1. Medusae with abnormal symmetry. Annotationes Zoologicae Japonenses 2, 373-376.

Uchida, T., 1929. Studies on the Stauromedusae and Cubomedusae, with special reference to their metamorphosis. Japanese Journal of Zoology 2, 103-193.

Uchida, T., 1973. The systematic position of the Stauromedusae. Publications of The Seto Marine Biological Laboratory 20, 133-139.

Uchida, T., Hanaoka, K.I., 1933. On the morphology of a stalked medusa, *Thaumatoscyphus distinctus* Kishinouye. Journal of the Faculty of Science Hokkaido Imperial University (Series VI. Zoology) 2, 135-153.

Van Iten, H., Leme, J.M., Simões, M.G., Marques, A.C., Collins, A.G., 2006. Reassessment of the phylogenetic position of conulariids (?Ediacaran- Triassic) within the subphylum Medusozoa (phylum Cnidaria). Journal of Systematic Palaeontology 4, 109-118.

Van Iten, H., Zhu, M. Y., Li, G.X., 2010. Redescription of Hexaconularia He and Yang, 1986 (Lower Cambrian, South China): Implications for the affinities of conulariid-like small shelly fossils. Palaeontology 53, 191-199.

Van Iten, H., Marques, A.C., Leme, J.M., Pacheco, M.L.A.F., Simoes, M.G., 2014. Origin and early diversification of the phylum cnidaria verrill: Major developments in the analysis of the taxon's Proterozoic-Cambrian history. Palaeontology 57, 677-690.

Vannier, J., Steiner, M., Renvoise, E., Hu, S.X., Casanova, J.P., 2007. Early Cambrian origin of modern food webs: evidence from predator arrow worms. Proc Biol Sci 274, 627-633.

Werner, B., 1972. Class Scyphozoan and Phylum Cnidaria In: Takasi Tokioka, S.N. (Ed.), The proceedings of the Scond International Symposium on Cnidaria, Shirahama and Kushimoto.

Werner, B., 1973. New investigations on systematics and evolution of the class Scyphozoa and the phylum Cnidaria. Publ. Seto Mar. Biol. Lab 20, 35-61.

Werner, B., Cutress, C.E., Studebaker, J.P., 1971. Life cycle of *Tripedalia cystophora* Conant (Cubomedusae). Nature 232, 582-583.

Xiao, S., Yuan, X., Knoll, A., 2000. Eumetazoan fossils in terminal Proterozoic phosphorites? Proceedings of the National Academy of Sciences of the United States of America 97, 13684.

Xu, Z.Z., Huang, J.Q., Lin, M., Guo, D., Wang, C.G., 2014. The Superclass Hydrozoa of the Phylum Cnidarian in China. China Ocean Press, Beijing (in Chinese).

Yao, X.Y, Han, J., Jiao, G., 2011. Early Cambrian epibolic gastrulation: A perspective from the Kuanchuanpu Member, Dengying Formation, Ningqiang, Shaanxi, South China. Gondwana Research 20, 844-851.

Yin, Z.J., Liu, P.J., Li, G., Tafforeau, P., Zhu, M.Y., 2014. Biological and taphonomic implications of
Ediacaran fossil embryos undergoing cytokinesis. Gondwana Research 25, 1019-1026.
doi:Doi 10.1016/J.Gr.2013.01.008.

Young, G.A., Hagadorn, J.W., 2010. The fossil record of cnidarian medusae. Palaeoworld 19, 212-221.

Yuan, X.L., Chen, Z., Xiao, S.H., Zhou, C.M., Hua, H., 2011. An early Ediacaran assemblage of
macroscopic and morphologically differentiated eukaryotes. Nature 470, 390-393.

Yue, Z., Bengtson, S., 1999. Embryonic and post-embryonic development of the Early Cambrian
cnidarian *Olivooides*. Lethaia 32, 181-195.

Zhang, X.L., Shu, D.G., Han, J., Zhang, Z.F., Liu, J.N., Fu, D.J., 2014. Triggers for the Cambrian
explosion: Hypotheses and problems. Gondwana Research 25, 896-909.

12. Figure Captions

**Figure 1. Pentamerous and tetramerous cubozoans from the Lower Cambrian
Kuanchuanpu Formation, Shaanxi, southern China.** (A-C) ELISN83-66. (A) Oral
view. (B-C) Reconstructions in aboral view (B) and lateral view (C); a piece of
apertural lappets was manually removed to expose the coronal muscles (crm). (D-E)
ELISN31-31. (D) Oral view showing two sets of the apertural lappets; (E), lateral
view, showing the coronal groove, apical interradial ridges and perradial furows. (F)
Pentamerous cubozoans (ELISN108-343), Ningqiang section. (G-I) ELISN131-38.
All photos except for (I) share the same scale bar as in (H) (200 μm).

Figure 2. Synchrotron X-ray micro-CT sections of a tetraradial cubozoan (ELISN83-66) from the Lower Cambrian Kuanchuanpu Formation, South China. (A) interradial and (B) perradial vertical sections with its oral side at the top. (C-T) Horizontal sections from bottom downward each corresponding to B'-T' in (A, B). All sections share the same scale bar (=300 µm), as in (C).

Figure 3. 3D rendering of the specimen ELISN83-66. (A) an oral view showing the disposition of the perradial and adradial apertural lappets (pal), and the manubrium (mb), some perradial and adradial apertural frenula are also visible as the incompleteness of the exumbrella. (B) A lateral view from the outside of the specimen, the meddle funnel (mf) and the coronal muscles (crm) are exposed due to the flaking of the exumbrella. (C) a lateral view of half specimen showing the exumbrella (eu), subumbrella (su), the short manubrium (mb) as well as the median funnel (mf), the subumbrellar wall are incompletely preserved thus a large portion of meddle funnel is exposed. (D) extraction of the perradial frenula (pfr) and a portion of coronal muscles (crm). (E) Perradial and adradial frenula and the tentacles. (F), the possible septal funnel extends longitudinally. (A)-(C), (E)-(F) share the same scale bars respectively.

Figure 4. Micro-CT sections of a tetramerous cubozoan (ELISN31-31) from the Lower Cambrian Kuanchuanpu Formation, South China. (A) interradial and (B) perradial vertical sections marked with a horizontal dotted line by A' and B' in (G). (C–L) Successive horizontal sections of the same specimen from the aboral pole upward, and their horizontal levels are marked by C'–L' in (A-B) with white dotted lines. All sections share the same scale bar (=200 μm) as in (L).

Figure 5. "Virtual"3D reconstructions of the specimen ELISN31-31. (A) an oral view showing the disposition of the perradial and adradial apertural lappets (pal), and the manubrium (mb). (B) an internal lateral view of half specimen showing the exumbrella (eu), subumbrella (su) as well as the manubrium. (C) a lateral external view showing the coronal groove, subapical circumferential groove (scg) and interradial ridges at the lower part. (D) a close-up lateral view of the deposition of the apertural lappets (pal) and frenula (pfr), please note the velarial canals (vc) are continuous with two lateral margins and the middle ridge of the perradial apertural lappet; the subumbrellar wall is much thinner than that of the exumbrella. (E) the subumbrella is concealed to show the gonad-lamellae (gl), the interradial septum is not shown here. (A)-(C) share the same scale bar.

Figure 6. Micro-CT sections of a cubozoan embryo (ELISN31-31) from the Lower Cambrian Kuanchuanpu Formation, South China. (A-B) Vertical sections respectively across interradius (A) and perradius (B). (C–L) Successive horizontal sections from the aboral pole upward, and their horizontal levels are marked by C'–L' in (A-B) with white dotted lines. All sections share the same scale bar (=100 μm) as in (L).

Figure 7. "Virtual"3D reconstructions of the specimen ELISN131-38. (A) an oral view showing the disposition of the perradial and adradial apertural lappets (pal), and the manubrium (mb). (B) a lateral view of half specimen showing the exumbrella (eu), subumbrella (su) as well as the median funnel (mf), the manubrium. (C) an aboral view showing the disposition of the interradial septa (is) and gonad-lamellae (gl). (D) a close-up lateral view of the perradial apertural lappets (pal) and underlying frenula (pfr). (E) subumbrella is removed to show the interradial septum (is) and gonad-lamellae (gl). (F) oral view of the central stomach cavity (csc). (A)-(C), (D)-(E) share the same scale bars respectively.

Figure 8. Schematic diagram of extant and fossil cubozoans. (A) a vertical and (B) a cross section of living *Charybdea xaymacana* Conant 1898 (Charybdeida, Cubozoa), modified from figures. 4 and 13 in (Conant, 1898). The perradial septa and the canals of sensory bulb are illustrated in (B). (C) the

40

pedalia are located outside the velarium in cubomedusae, such as living *Chironex yamaguchii* Lewis & Bentlage 2009 (Cubozoa: Chirodropida). (D) Close-up of (C) showing the coronal muscles. (E) Reconstructions of the cross section of a pentamerous cubozoan (specimen ELISN108-343 in Han et al., 2013) at the horizontal level of tentacles. F–G, Reconstructions of the cross sections of ELISN-31-31. (F). Correspond to Fig. 4I, showing the well-separated paired tentacles. (G) Correspond to Fig. 4G, showing the endodermic perradial fusion as perradial septa.

Figure 9 Strict consensus of three most parsimonious trees resulting from the cladistic analysis of medusozoan relationships based on 25 taxa and 104 characters through successive weighting. Tree length=94.73492, Consistency index (CI)=0.875, Homoplasy index (HI)=0.125, Rescaled consistency index (RC)=0.807.

Figure 10. Hypothesis on the symmetric patterns of medusozoans. The divergence times of bilaterians and major cnidarian clades come respectively from the refs (Shu et al., 2014 and Park et al., 2011).
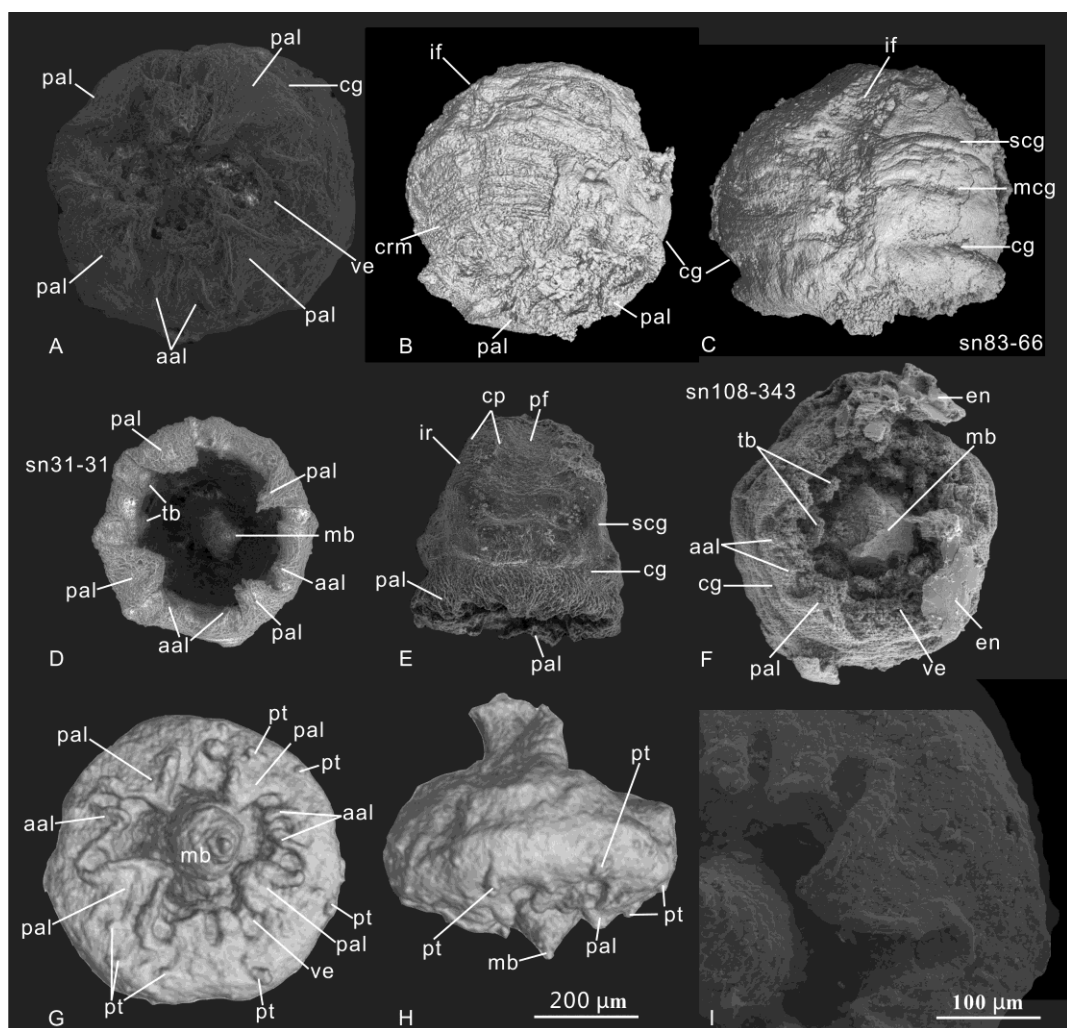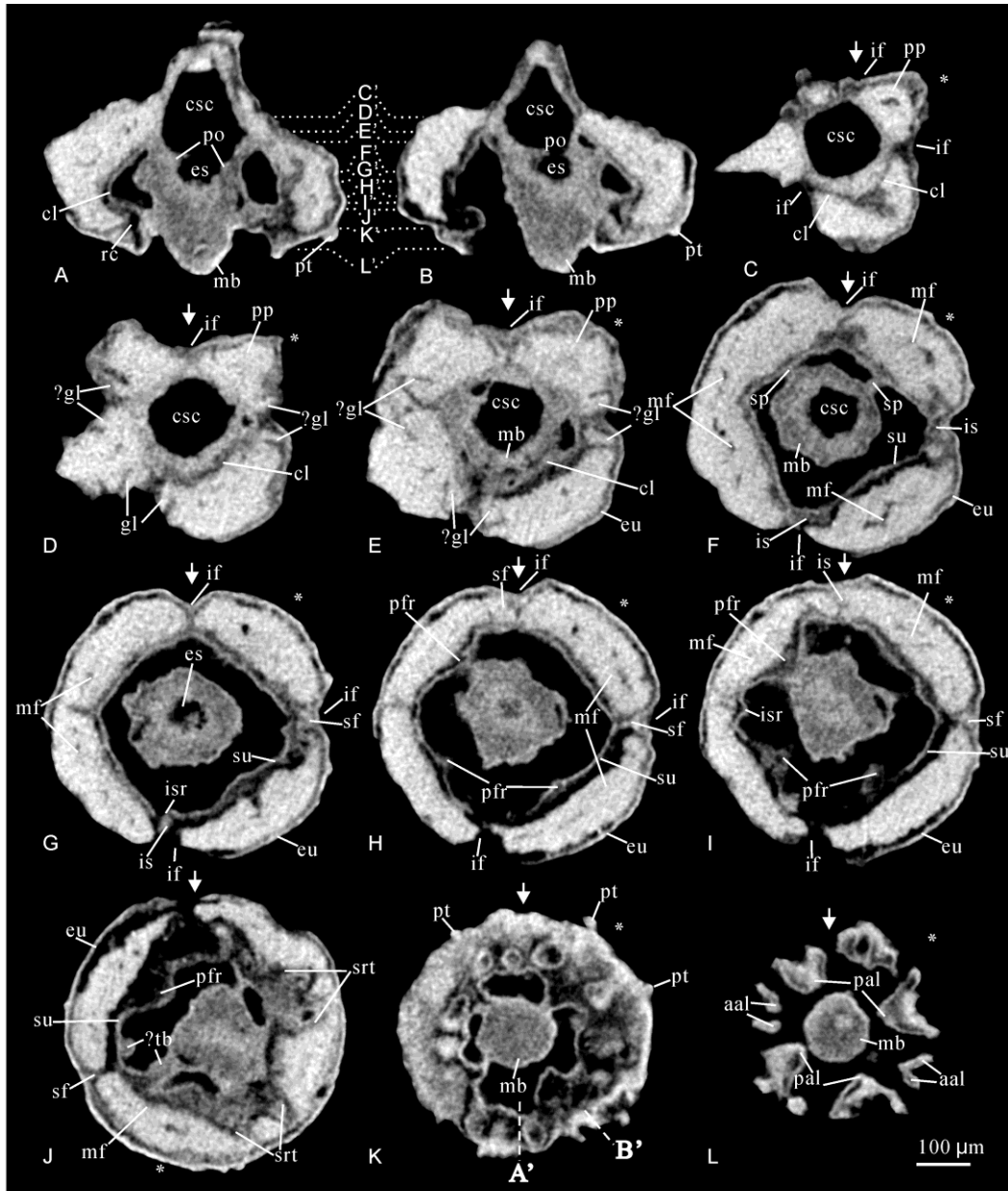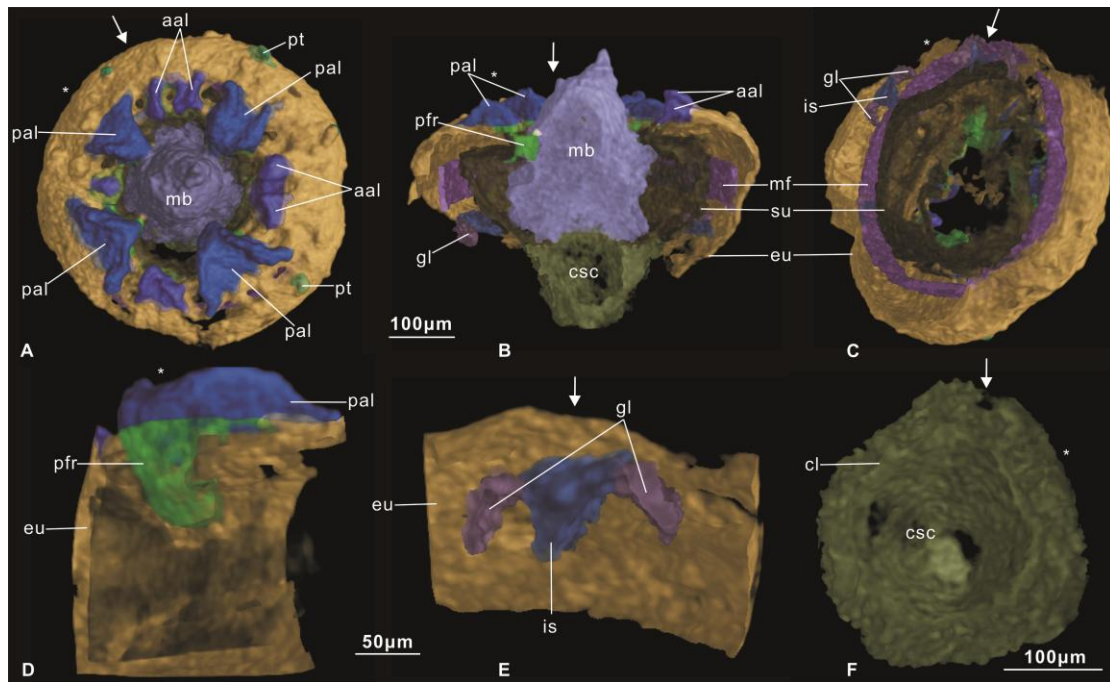
Figure 1
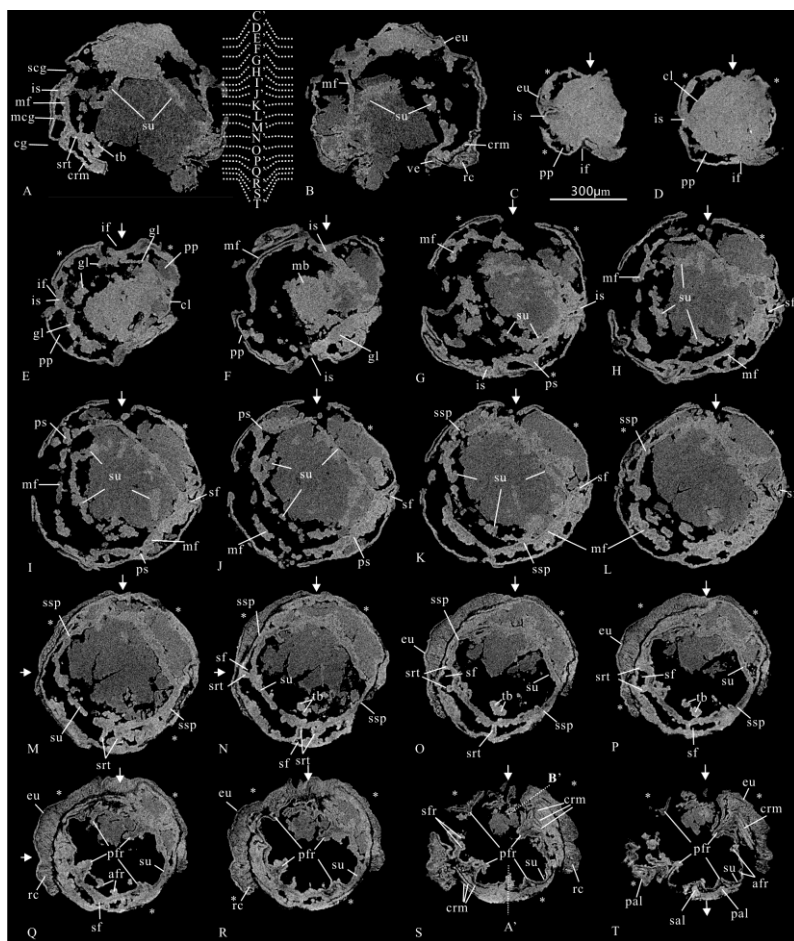
Figure 2
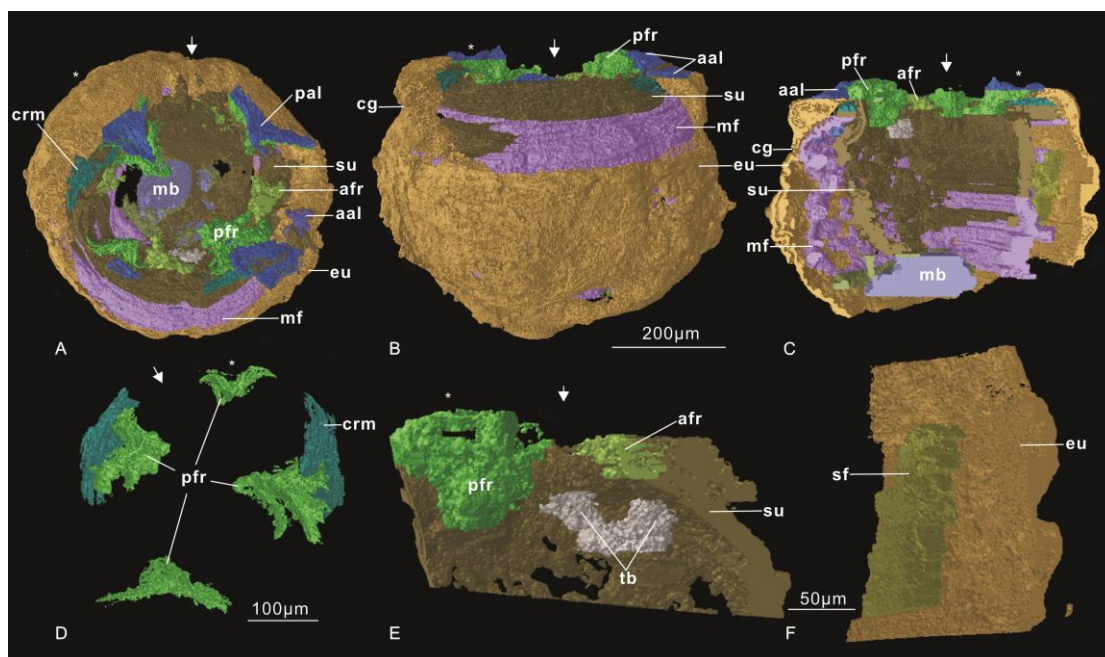
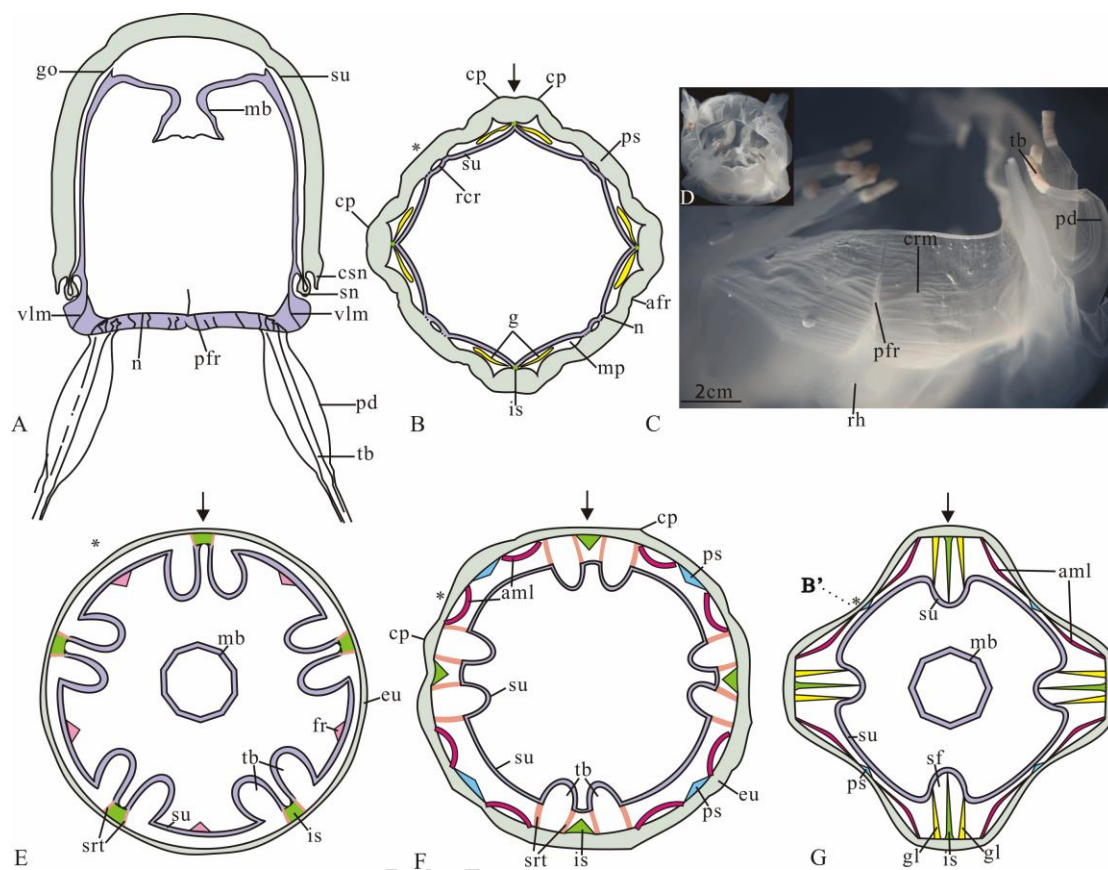Figure 3
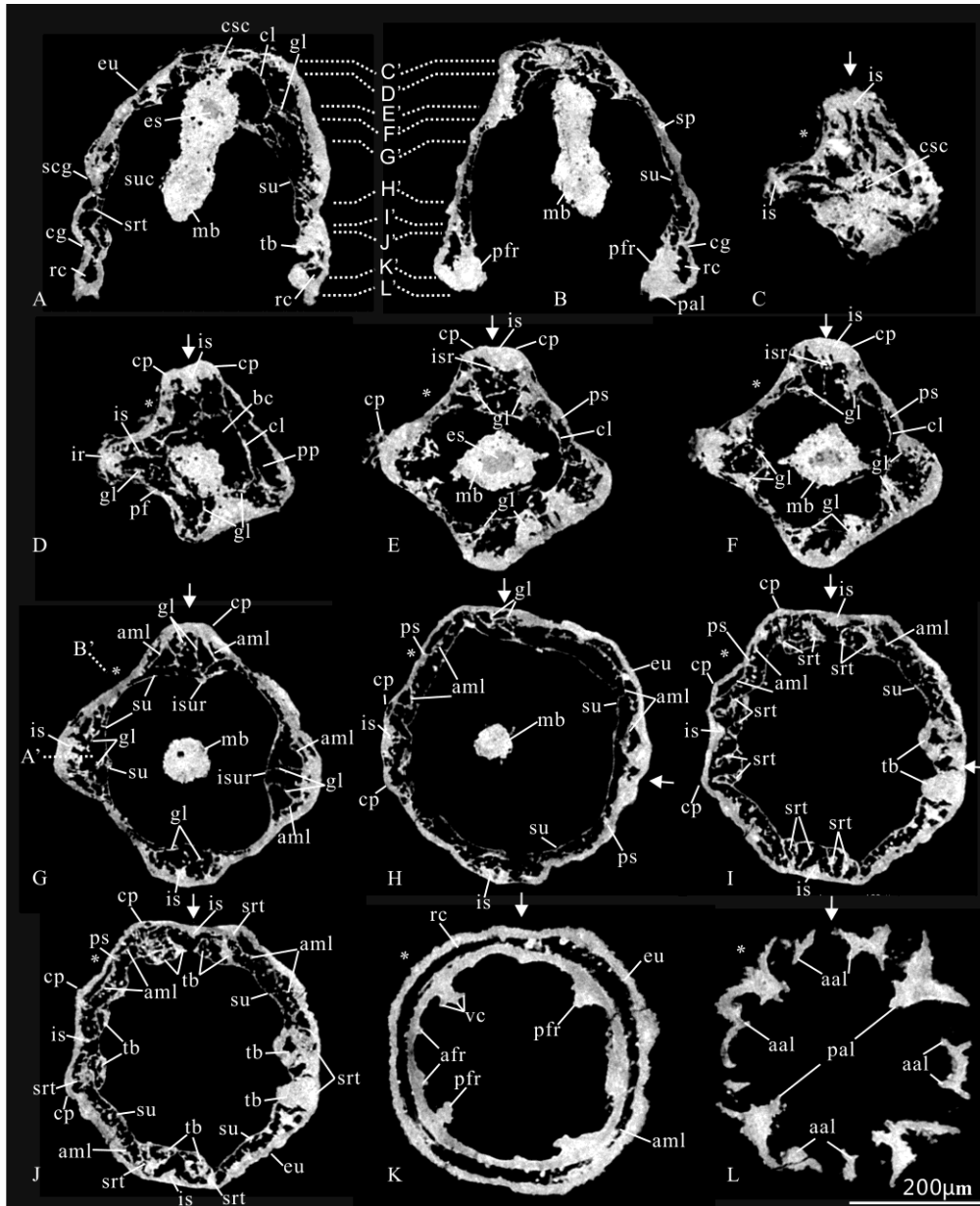
Figure 4
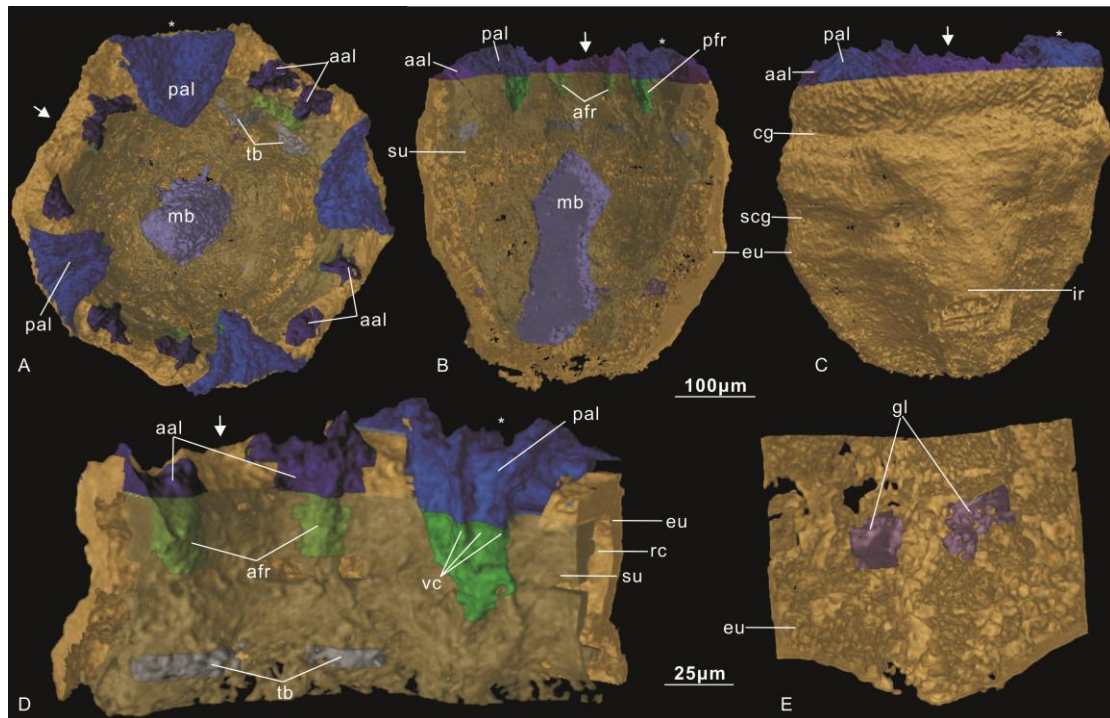
Figure 5

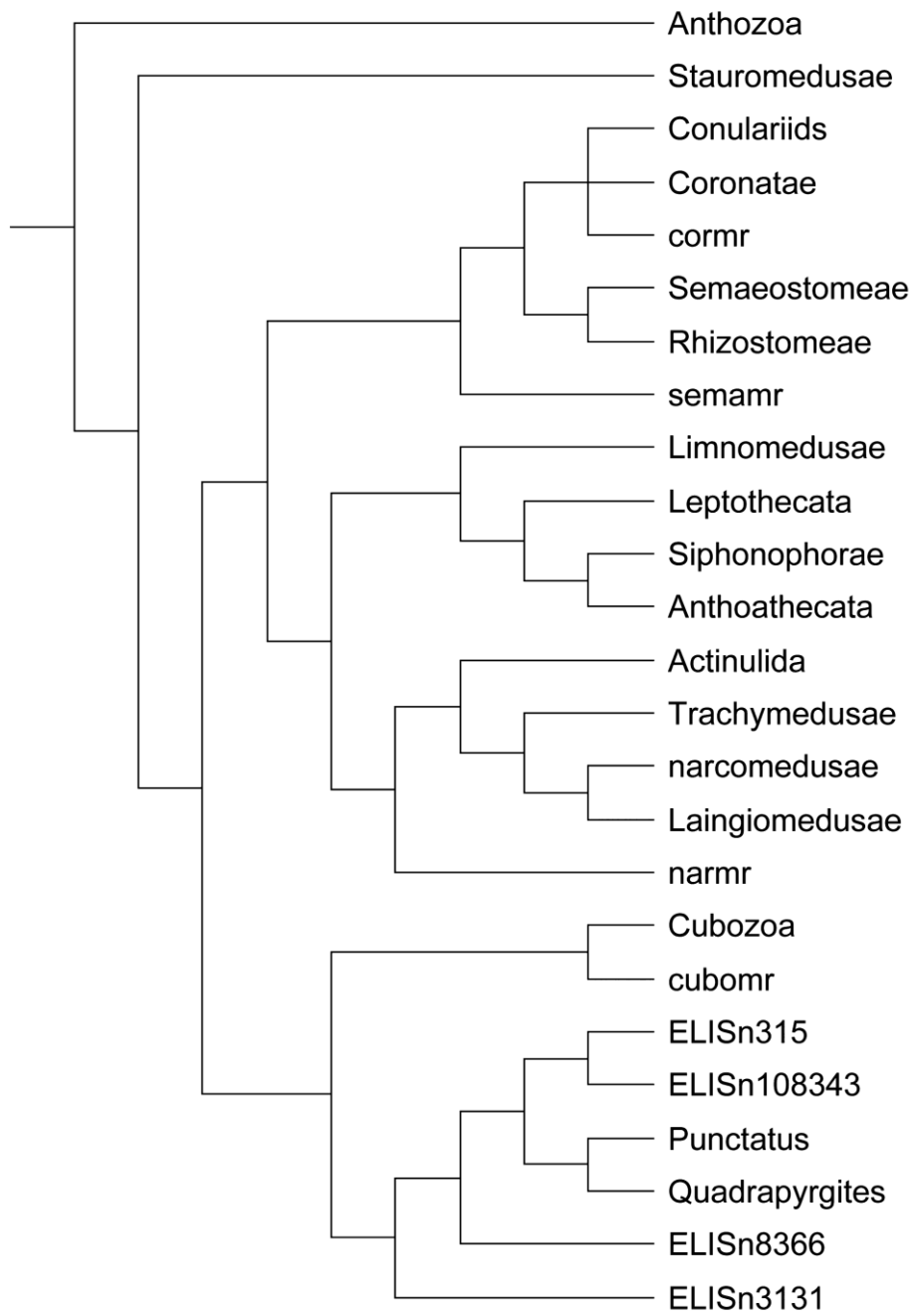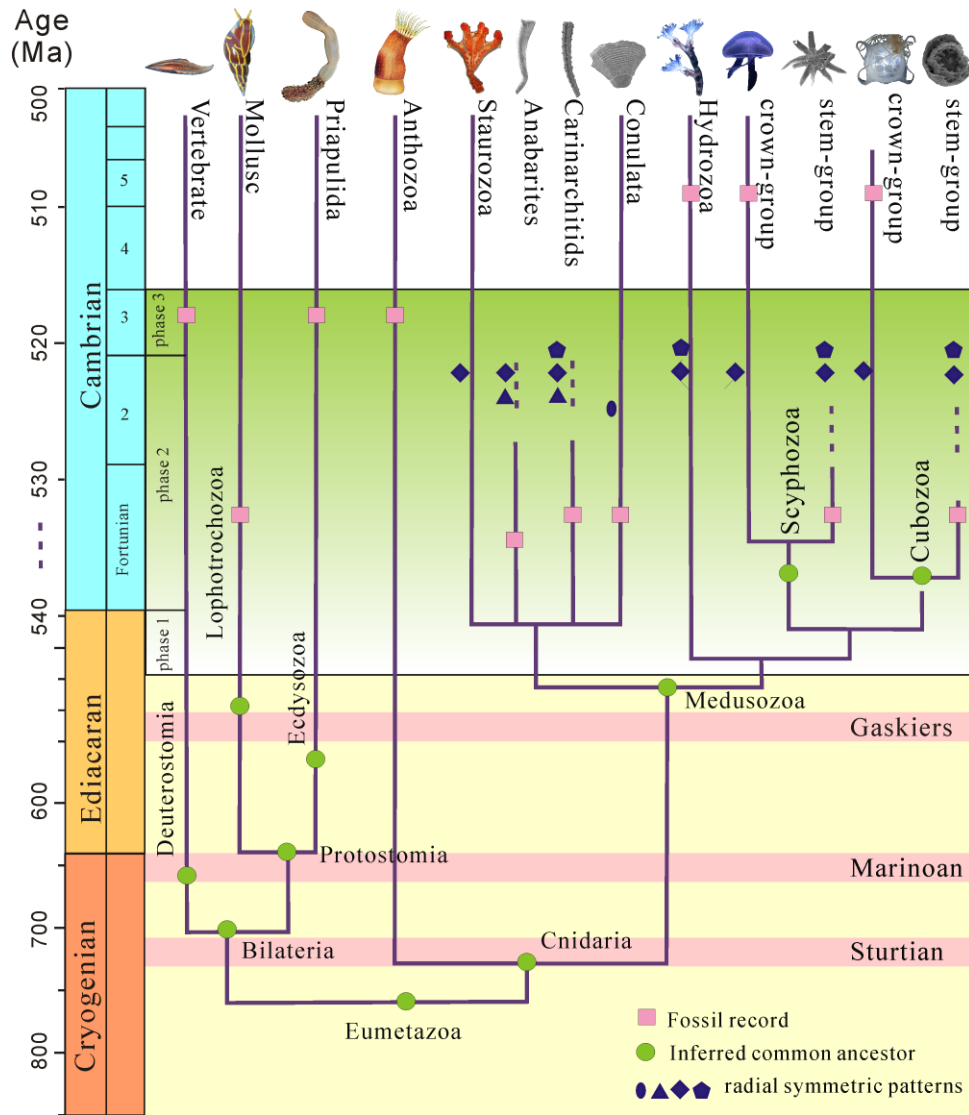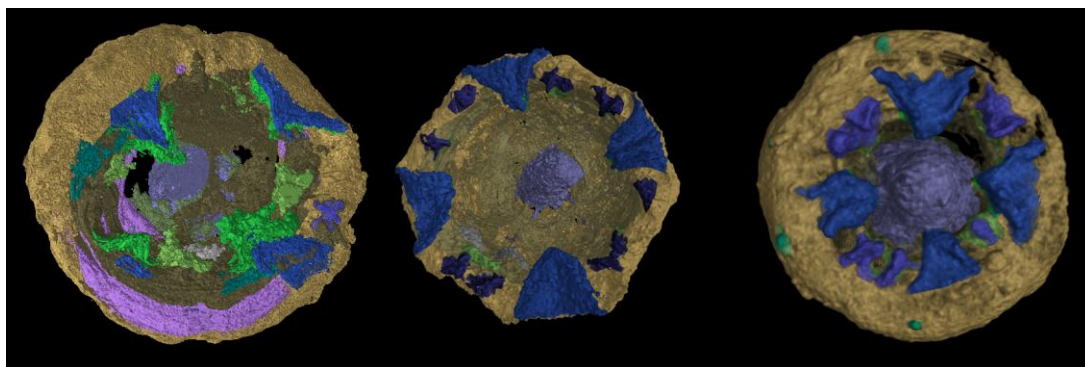Figure 6

Figure 7

Figure 8

Figure 9

Figure 10

Graphical abstract

Research highlights:

► First report of tetramerous cubozoan fossils from the earliest Cambrian

► These fossils display well preserved soft-tissue and internal anatomy

► Corner pillars and perradial fusion are critical for shaping box jellyfish

► Tetra- and penta-radiated fossils belong to a monophyletic stem-group cubozoan

► There are diverse symmetric patterns among Cambrian medusozoans.